Separation Science and Technology
Publication details, including instructions for authors and subscription information:
http://www.informaworld.com/smpp/title~content=t713708471

Modeling of the Permeation of Copper through Liquid Surfactant Membranes

Masaaki Teramoto[a]; Tsutomu Sakai[a]; Kouyou Yanagawa[a]; Motoyuki Ohsuga[a]; Yoshikazu Miyake[a]
[a] DEPARTMENT OF INDUSTRIAL CHEMISTRY, KYOTO INSTITUTE OF TECHNOLOGY MATSUGASAKI, KYOTO, JAPAN

To cite this Article Teramoto, Masaaki , Sakai, Tsutomu , Yanagawa, Kouyou , Ohsuga, Motoyuki and Miyake, Yoshikazu(1983) 'Modeling of the Permeation of Copper through Liquid Surfactant Membranes', Separation Science and Technology, 18: 8, 735 — 764

To link to this Article: DOI: 10.1080/01496398308068577

URL: http://dx.doi.org/10.1080/01496398308068577

SEPARATION SCIENCE AND TECHNOLOGY, 18(8), pp. 735–764, 1983

Modeling of the Permeation of Copper through Liquid Surfactant Membranes

MASAAKI TERAMOTO,* TSUTOMU SAKAI,
KOUYOU YANAGAWA, MOTOYUKI OHSUGA,
and YOSHIKAZU MIYAKE

DEPARTMENT OF INDUSTRIAL CHEMISTRY
KYOTO INSTITUTE OF TECHNOLOGY
MATSUGASAKI, SAKYO-KU, KYOTO 606, JAPAN

Abstract

A general permeation model for the extraction of copper by liquid surfactant membranes using a chelating agent as a carrier is presented in which the internal mass transfer in the W/O emulsion drop, the external mass transfer around the drop, the rates of the formation and decomposition of the complex at the aqueous–organic interface, and the leakage of the internal aqueous phase to the external phase due to the membrane breakup are taken into account. The batch extraction of copper using SME529 as a carrier was carried out under various experimental conditions. It is shown that the extraction rates can be satisfactorily simulated by the present model.

INTRODUCTION

A separation technique using liquid surfactant membranes, first developed by Li (*1*) for the selective permeation of hydrocarbons in 1968, has been noted as a novel method for an increasingly wide variety of separations including the separation of hydrocarbons (*2–9*) and the removal and/or recovery of phenol (*10–13*) and amines (*14, 15*). Since Cussler (*16*) demonstrated that sodium ion could be pumped against its concentration gradient by introducing a carrier which reacts with the solute reversibly into supported liquid membranes, special attention has been paid to the

---

*To whom correspondence should be addressed.

0149-6395/83/1808-0735$3.50/0

concentrations of various metal ions by use of the active transport mechanism (*14*, *17–25*). While a number of papers have shown experimentally the possibility of applying the liquid surfactant membrane process to the separation of metal ions, very few papers have dealt with the permeation rate through membranes quantitatively because of their very complicated geometrical configuration. Hochhauser et al. (*17*), Martin et al. (*19*), and Völkel et al. (*22*) presented a model in which mass transfer resistance is localized in the peripheral oil layer of the W/O emulsion drop, and the mass transfer resistance in the W/O emulsion drop is neglected to simplify the mathematical treatment. However, this model cannot account for the effect of the concentration of the internal reagent on the extraction rate, as described later. On the other hand, Marr et al. (*25*) proposed a shrinking core model for the extraction of copper using LIX 64N as a carrier. They considered that the internal droplets are immobile and there exists a sharp boundary between the outer region saturated with copper and the inner unsaturated region, and this boundary moves toward the center of the W/O emulsion drop as the extraction proceeds. In their analysis, however, the change of the copper-carrier complex concentration at the external surface of the emulsion drop during the extraction was not considered. Furthermore, the external aqueous phase mass transfer resistance, which might be more important than the internal mass transfer resistance in the early stage of the extraction or in the extraction of copper of low concentration, was not taken into account.

The present author proposed a general mass transfer model for the extraction of weak bases such as ammonia and amines (*13*), and weak acids such as phenol and cresol (*15*) by liquid surfactant membranes in which the diffusion in the W/O emulsion drops, the external mass transfer, and both the chemical and phase equilibria were taken into account. In this paper, this model is extended to the extraction of copper by liquid surfactant membranes containing a chelating agent as a carrier. It is shown that the effects of various experimental conditions on the permeation rate of copper through membranes containing SME529 as a carrier can be quantitatively explained by the proposed model.

THEORY

Here, it is assumed that the mass transfer resistance in the internal aqueous phase is neglected because of the very small size of the internal droplet, and also that a monobasic acid such as hydrochloric acid and nitric acid is used as the internal stripping agent.

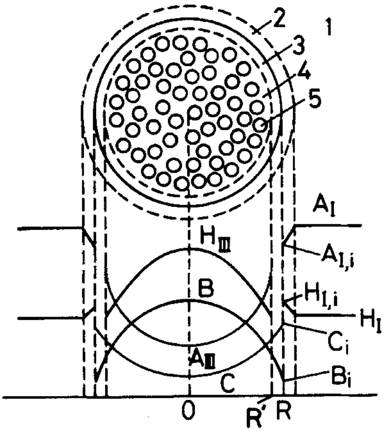

FIG. 1. Schematic diagram of W/O/W multiphase emulsion system: (1) External aqueous phase (Phase I), (2) stagnant film of Phase I around emulsion drop, (3) peripheral oil layer, (4) oil membrane phase (Phase II), (5) internal aqueous phase (Phase III).

As shown in Fig. 1, the elementary steps of copper permeation through the liquid membrane are as follows.

1. (1) Diffusions of copper and hydrogen ions through the stagnant film of the external aqueous phase.
2. (2) Complex formation between Cu^{2+} and HR, the chelating agent, at the external interface of the W/O emulsion drop.
3. (3) Diffusions of the complex and the chelating agent in the peripheral oil layer of the emulsion drop.
4. (4) Diffusions of the complex and the chelating agent through the interstitial oil membrane phase.
5. (5) Stripping of copper at the interface between the oil membrane phase and the internal aqueous phase droplets containing hydrochloric acid.

It has been already found that the reaction between Cu^{2+} and anti-2-hydroxy-5-tert-nonylacetophenone oxime, the active species of SME529, occurs at the organic–aqueous interface, and also that the forward and the reverse reaction rates are represented as follows (*26, 27*):

$$Cu^{2+} + 2HR \rightleftharpoons CuR_2 + 2H^+ \tag{1}$$

$$(A + 2B \rightleftharpoons C + 2H)$$

$$K_{ex} = ([\mathrm{CuR_2}][\mathrm{H^+}]^2/[\mathrm{Cu^{2+}}][\mathrm{HR}]^2)_{eq} = (CH^2/AB^2)_{eq} \tag{2}$$

$$r_f = k_f(AB/H - CH/K_{ex}B) \tag{3}$$

$$r_r = k_r(CH - K_{ex}AB^2/H) \tag{4}$$

The mass balance equation of copper in the external aqueous phase is represented by

$$(1 - \phi')\partial A_{\mathrm{I}}/\partial t = -k_A a_0(A_{\mathrm{I}} - A_{\mathrm{I},i}) + (v_b/V_T)(A_{\mathrm{III}})_{r=R'} \tag{5}$$

where k_A is the mass transfer coefficient of $\mathrm{Cu^{2+}}$ through the aqueous film and a_0 the specific surface area of W/O emulsion phase ($= S/V_T$), and ϕ' the volume fraction of drops $[= (V_{\mathrm{II}} + V_{\mathrm{III}})/V_T]$. V_{I}, V_{II}, and V_{III} are the volumes of the external aqueous phase (Phase I), the membrane phase (Phase II), and the internal aqueous phase (Phase III), respectively, and V_T is the total volume ($= V_{\mathrm{I}} + V_{\mathrm{II}} + V_{\mathrm{III}}$). S is the interfacial area between the external aqueous phase and the W/O emulsion drops, and v_b is the volumetric rate of the leakage of Phase III to Phase I due to the breakage of the membrane. The last term in Eq. (5) represents the transfer rate of copper from the internal phase to the external feed solution due to the membrane breakup. Here, it is assumed that the internal droplets at the peripheral region of the W/O emulsion drop leak. The validity of this assumption will be discussed later.

The mass balance equations of the chelating agent B and the complex C in the region of $0 \le r \le R'$ in the emulsion drop are expressed by

$$(1 - \phi)\frac{\partial B}{\partial t} = D_{e,B}\left(\frac{\partial^2 B}{\partial r^2} + \frac{2}{r}\frac{\partial B}{\partial r}\right) + \frac{6\phi k_r}{R_\mu}\left(CH_{\mathrm{III}} - \frac{K_{ex}A_{\mathrm{III}}B^2}{H_{\mathrm{III}}}\right) \tag{6}$$

$$(1 - \phi)\frac{\partial C}{\partial t} = D_{e,C}\left(\frac{\partial^2 C}{\partial r^2} + \frac{2}{r}\frac{\partial C}{\partial r}\right) - \frac{3\phi k_r}{R_\mu}\left(CH_{\mathrm{III}} - \frac{K_{ex}A_{\mathrm{III}}B^2}{H_{\mathrm{III}}}\right) \tag{7}$$

Here, ϕ is the volume fraction of the internal aqueous phase in the emulsion drop $[= V_{\mathrm{III}}/(V_{\mathrm{II}} - V_{\mathrm{III}})]$. The mass balance equation of copper in the internal aqueous phase is

$$\phi \partial A_{\rm III}/\partial t = (3\phi k_r/R_\mu)(CH_{\rm III} - K_{ex}A_{\rm III}B^2/H_{\rm III}) \tag{8}$$

Here, R_μ denotes the Sauter mean diameter of the internal aqueous phase droplets, and $3\phi/R_\mu$ corresponds to the interfacial area between the membrane and the internal droplets per unit volume of the W/O emulsion. Hereafter, the "drop" refers to the W/O emulsion drop dispersed in Phase I, and the "droplet" the internal droplet. The initial and the boundary conditions are as follows.

I.C.;

$$A_{\rm I} = A_{\rm I,0} \qquad \text{for } t = 0 \tag{9}$$

$$B = B_0,\ C = C_0,\ A_{\rm III} = A_{\rm III,0},\ (H_{\rm III} = H_{\rm III,0}) \qquad \text{for } 0 \le r \le R',\ t = 0 \tag{10}$$

B.C.1;

$$\partial B/\partial r = \partial C/\partial r = 0 \qquad \text{for } r = 0,\ t \ge 0 \tag{11}$$

B.C.2;

$$\begin{aligned} k_A(A_{\rm I} - A_{{\rm I},i}) &= k_H(H_{{\rm I},i} - H_{\rm I})/2 \\ &= k_f(A_{{\rm I},i}B_i/H_{{\rm I},i} - C_iH_{{\rm I},i}/K_{ex}B_i) \\ &= k_B\{(B)_{r=R'} - B_i\}/2 \\ &= k_C\{C_i - (C)_{r=R'}\} \\ &= -D_{e,B}(\partial B/\partial r)_{r=R'}/2 \\ &= D_{e,C}(\partial C/\partial r)_{r=R'} \end{aligned} \tag{12}$$

Here, k_B and k_C are the mass transfer coefficients of B and C through the peripheral oil layer, respectively. In the internal aqueous phase, the following relation holds:

$$2A_{\rm III,0} + H_{\rm III,0} = 2A_{\rm III} + H_{\rm III} \tag{13}$$

The above equations are transformed to dimensionless forms by the use of the variables and parameters given by Eq. (14):

$$\frac{\partial y}{\partial \theta} = -\{3\phi' Bi/(1-\phi')\}(y - y_i) + \frac{\alpha Bi m_{H,\rm III}}{2m_{A,\rm I}(1-\phi')}(w)_{x=1} \tag{5'}$$

$$(1-\phi)\frac{\partial b}{\partial \theta} = \left(\frac{\partial^2 b}{\partial x^2} + \frac{2}{x}\frac{\partial b}{\partial x}\right) + 3\phi Biqz \tag{6'}$$

$$(1-\phi)\frac{\partial c}{\partial \theta}=r_{CB}\left(\frac{\partial^2 c}{\partial x^2}+\frac{2}{x}\frac{\partial c}{\partial x}\right)-3\phi Biqz \tag{7'}$$

$$\partial w/\partial \theta = 3Biqz/m_{H,\text{III}} \tag{8'}$$

where

$$z = c(1+m_{A,\text{III}}/m_{H,\text{III}}-w)-\frac{K_{ex}b^2 w}{m_{H,\text{III}}(1+m_{A,\text{III}}/m_{H,\text{III}}-w)}$$

I.C.; $y = 1$ for $\theta = 0$ (9′)

$b = 1,\ c = c_0,\ w = w_0$ for $0 \leqq x \leqq 1,\ \theta \geqq 0$ (10′)

B.C.1; $\partial b/\partial x = \partial c/\partial x = 0$ for $x = 0,\ \theta \geqq 0$ (11′)

B.C.2; $y - y_i = (k_H/k_A)(H_{\text{I},i}-H_\text{I})/(2A_{\text{I},0})$

$$\begin{aligned} &= n_f\left[\frac{y_i b_i}{m_{H,i}(H_{\text{I},i}/H_{\text{I},0})}-\frac{m_{H,\text{I}}(H_{\text{I},i}/H_{\text{I},0})c_i}{2K_{ex}b_i m_{A,\text{I}}}\right] \\ &= (n_B/2m_{A,\text{I}})\{(b)_{x=1}-b_i\} \\ &= (n_C/2m_{A,\text{I}})\{c_i-(c)_{x=1}\} \\ &= -(\partial b/\partial x)_{x=1}/(2Bim_{A,\text{I}}) \\ &= (\partial c/\partial x)_{x=1}(r_{CB}/2Bim_{A,\text{I}}) \end{aligned} \tag{12'}$$

$$(m_{A,\text{III}}/m_{H,\text{III}})+1 = w + H_\text{III}/H_{\text{III},0} \tag{13'}$$

$$\begin{aligned} &y = A_\text{I}/A_{\text{I},0},\ b = B/B_0,\ c = 2C/B_0,\ w = 2A_\text{III}/H_{\text{III},0},\ Bi = k_A R/D_{e,B}, \\ &m_{A,\text{I}} = A_{I,0}/B_0,\ m_{A,\text{III}} = 2A_{\text{III},0}/B_0,\ m_{H,\text{I}} = H_{\text{I},0}/B_0, \\ &m_{H,\text{III}} = H_{\text{III},0}/B_0,\ n_B = k_B/k_A,\ n_C = k_C/k_A,\ n_f = k_f/k_A, \\ &q = Rk_r H_{\text{III},0}/R_\mu k_A,\ r_{CB} = D_{e,C}/D_{e,B},\ \alpha = Rv_b/k_A V_T \end{aligned} \tag{14}$$

Here, it is assumed that R' is approximately equal to R. Another equation describing the change of H_I is necessary to complete the basic equations. In this study, however, this was not considered because buffer solutions were used in most of the experiments. Therefore, mass transfer resistance of H^+ in the external stagnant film was not considered.

If 14 parameters (α, ϕ, ϕ', Bi, $m_{A,\mathrm{I}}$, $m_{A,\mathrm{III}}$, $m_{H,\mathrm{I}}$, $m_{H,\mathrm{III}}$, n_B, n_C, n_f, q, K_{ex}, and r_{CB}) are given, the basic equations can be numerically solved. Here, the finite difference method was used. Although this analysis assumes uniform drop size distribution of W/O emulsion, it can be extended to the case where drop size distribution exists (*13*), as will be described later.

EXPERIMENTAL

The experimental apparatus used was the same as reported in previous papers (*13*, *15*). The W/O emulsion was prepared as follows. A mixture of 50 cm^3 of Dispersol, a sort of kerosene offered by Shell Chemical Co. Ltd., containing Span 80 (sorbitan monooleate) and SME529 (Shell Chemical Co. Ltd.), and the same volume of aqueous solution of hydrochloric acid and lithium chloride, and the tracer to measure the degree of leakage of the internal phase to the external phase due to the breakage of the membrane were agitated for 15 min by a vibromixer. Then the mixture was sonicated by an ultrasonic homogenizer. A portion of the W/O emulsion thus prepared was dispersed in the agitation vessel containing 600 cm^3 of buffer solution, a mixture of the solutions 0.5 *M* CH_3COOH and 0.5 *M* CH_3COONa. The vessel was 9 cm in diameter and equipped with a six-bladed turbine agitator. In about 3 min, an aqueous solution of cupric sulfate was introduced into the vessel to start the extraction. The total volume of the external aqueous phase was 650 cm^3, and the volume of the W/O emulsion ranged from 18 to 100 cm^3. Samples were drawn from the external phase, and the copper concentration was analyzed by an atomic absorption spectrophotometer. Lithium concentration was determined by a flame emission spectrophotometer. The fraction of leakage, *f*, which is defined as the ratio of the volume of the internal phase which leaks to the external phase to the initial volume of the internal phase, was calculated by

$$f = (1 - \phi')[\mathrm{Li}^+]_{\mathrm{I}}/(\phi\phi'[\mathrm{Li}^+]_{\mathrm{III},0}) \qquad (15)$$

The drop size distributions of the W/O emulsion and the internal aqueous phase were measured by the photographic and the microscopic methods, respectively. Unless otherwise stated, the concentration of Span 80 was 5 vol%, the stirring speed was 300 rpm, the temperature was 298 K, and the initial concentration of the copper in Phase III was 0.

RESULTS

Estimation of Parameters

Of many parameters included in the present model, $m_{A,\mathrm{I}}$, $m_{A,\mathrm{III}}$, $m_{H,\mathrm{I}}$, $m_{H,\mathrm{III}}$, ϕ, and ϕ' can be easily calculated from the experimental conditions. It is desirable to determine other parameters independently. For this purpose a series of experiments was carried out.

The values of k_A and k_f were obtained as follows. The rate-determining step of copper extraction changes depending on the experimental condition. It was found that under the condition that $A_{\mathrm{I},0}$ is low compared with B_0, the rate is limited by the diffusion of copper through the external aqueous stagnant film if H_I is sufficiently low, and by the reaction at the interface of the emulsion drop if H_I is high. When the reverse reaction is ignored, the extraction rate is expressed as follows.

$$-V_\mathrm{I}dA_\mathrm{I}/dt = k_AS(A_\mathrm{I} - A_{\mathrm{I},i}) = k_fSA_{\mathrm{I},i}B_i/H_\mathrm{I}$$
$$\cong A_\mathrm{I}S/(1/k_A + H_\mathrm{I}/k_fB_0) = K_ASA_\mathrm{I} \tag{16}$$

Integration of Eq. (16) gives

$$\ln(A_\mathrm{I}/A_{\mathrm{I},0}) = \ln y = -\{K_Aa_0/(1-\phi')\}t = -[3K_A\phi'/\{(1-\phi')R\}]t \tag{17}$$

where

$$1/K_A = 1/k_A + H_\mathrm{I}/k_fB_0 \tag{18}$$

Experiments were carried out at various hydrogen ion concentrations with other conditions kept constant. As shown in Fig. 2, the plot of ln y vs t gives straight lines, and K_A's are calculated from their slopes. Figure 3 indicates that the plot of $1/K_A$ against H_I also gives a straight line in accordance with Eq. (18). The values of k_A and k_f can be calculated from its intercept and slope, respectively (see Table 1). The value of k_A approximately agrees with the value of k_A, 0.0023, estimated using the equation by Calderbank and Moo-Young (*28*). The value of k_f was 1.6×10^{-5} cm/s when the pH of the external phase was considerably high. However, it was 1.0×10^{-5} at low pH where pH was adjusted by adding hydrochloric acid without using the buffer solution. This is probably because, depending on the species of coexisting anion in the external phase, copper exists in a different form of the copper complex, having a different reactivity toward the carrier.

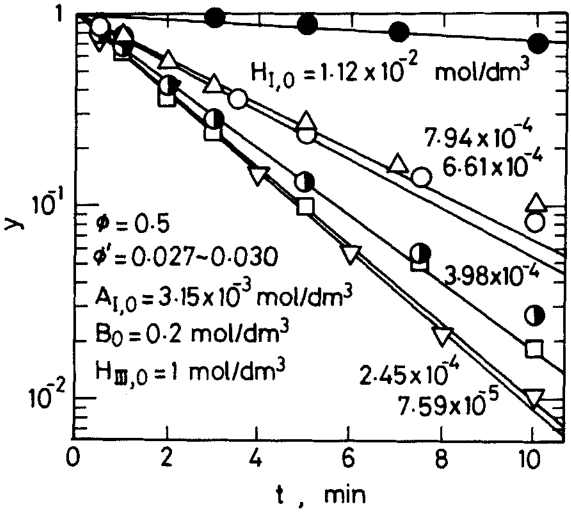

FIG. 2. Determination of K_A as a function of $H_{I,0}$.

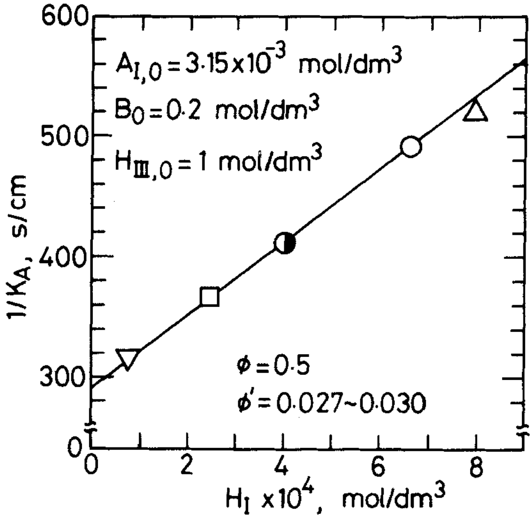

FIG. 3. Plot of $1/K_A$ vs H_I.

TABLE 1
Values of Parameters

$D_{e,B}$:	$2.29 \times 10^{-6}/\mu$ cm^2/s, μ:cP	K_{ex}:	0.6
k_A:	0.0034 cm/s	k_B:	0.0004 cm/s
k_C:	0.00264 cm/s	k_f:	1.0×10^{-5}–1.6×10^{-5} cm/s
k_r:	0.044 cm^4/mol · s	r_{CB}:	0.66

It was impossible to determine k_B or k_C in the W/O/W multiphase system. However, a rough estimate was made by the extraction experiment using an agitation vessel, 7 cm in diameter and 14 cm in height, equipped with a 6-bladed turbine agitator. 200 cm^3 of the aqueous copper solution was first introduced into the vessel. Then 100 cm^3 of the W/O emulsion phase was carefully poured over the aqueous phase so as not to disturb the interface. Stirring in the emulsion phase was started at 100 rpm, and samples were taken from the aqueous phase for analysis. Under the condition that $A_{\mathrm{I},0}$ was sufficiently high and $H_{\mathrm{I},0}$ was considerably low, the resistances of the aqueous stagnant film diffusion and the interfacial reaction could be neglected. It was also anticipated that the diffusion rate of the complex in the emulsion phase would be fast due to the convection caused by agitation. Thus, the rate-determining step was the diffusion of the complex and the carrier through the oil layer adjacent to the interface. The experimental result is shown in Fig. 4. The copper concentration in the aqueous phase decreased linearly with time, suggesting that the rate of extraction was independent of copper concentration. This means that on the aqueous side of the oil layer, almost all of the carrier was consumed by complexation with copper. Thus, the extraction rate is expressed by

$$-V_{\mathrm{I}} dA_{\mathrm{I}}/dt = k_B S(B_0 - B_i)/2 = k_B S(B_0 - 0)/2 \qquad (19)$$

From Eq. (19) and the data shown in Fig. 4, the value of k_B was calculated. The value of k_C was estimated using the relation $k_C = k_B(D_C/D_B)$. As shown in Table 1, these values are relatively small. The diffusivity of B, estimated by the Wilke-Chang equation (*29*), was 2.48×10^{-6} cm^2/s. Then the oil layer thickness calculated from $\delta = D_B/k_B$ was 62 μm. This large value of δ may be explained as follows. In the kinetic study on the extraction of copper by SME529 using a Lewis cell, the present authors found that the organic phase mass transfer coefficient of SME529 was as low as 8.9×10^{-5} cm/s and about one-third of that of phenol. This discrepancy could not be explained by the difference in their diffusivities (*26*). Although a clear conclusion could not be drawn, it was deduced that the slow adsorption rate

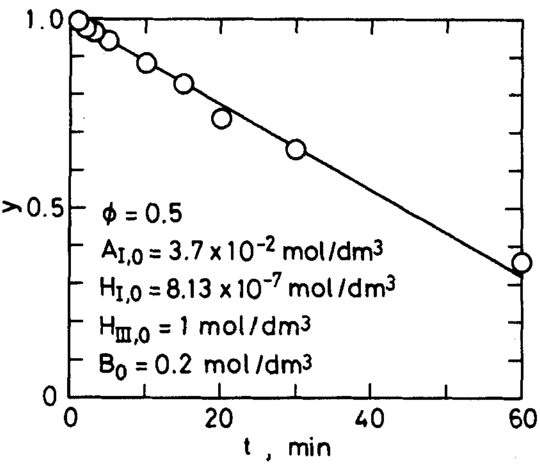

FIG. 4. Determination of k_B.

of SME529 at the aqueous–organic interface might be the cause of the low value of k_B and, in turn, the high value of δ. The actual value of δ may be much smaller.

K_{ex} was determined from the distribution ratio of copper between the aqueous and organic phase measured by the usual method. The value of k_r was determined using a Lewis cell under the conditions of interfacial reaction rate controlling (*27*).

The value of v_b was obtained as follows. The plot of f against t is shown in Fig. 5. Considerable leakage was observed when the emulsion was dispersed at the start of the extraction, and f increased linearly with time. v_b was calculated as the product of the slope and V_{III}.

The effective diffusivities $D_{e,B}$ and $D_{e,C}$ were determined so that the computed results might agree with the experimental results. It was assumed that the ratio $D_{e,C}/D_{e,B}$ is equal to the bulk diffusivity ratio, D_C/D_B.

Effect of Experimental Conditions on the Extraction Rate

Effect of Copper Concentration in the Feed Solution

Figure 6 shows the effect of the initial concentration of copper in the feed solution on the time course of extraction when the interfacial reaction rate is fast, i.e., the hydrogen ion concentration is very low. It is seen that the higher

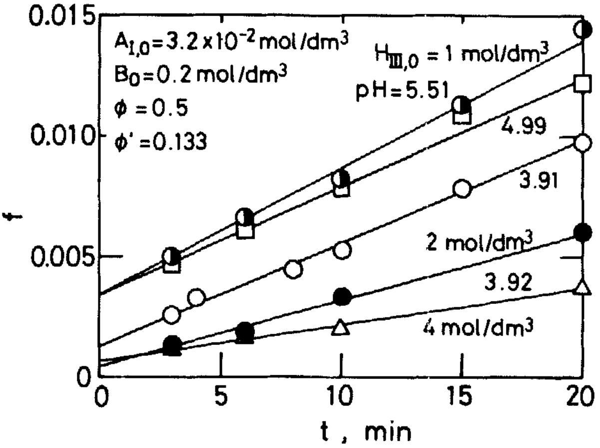

FIG. 5. Determination of v_b.

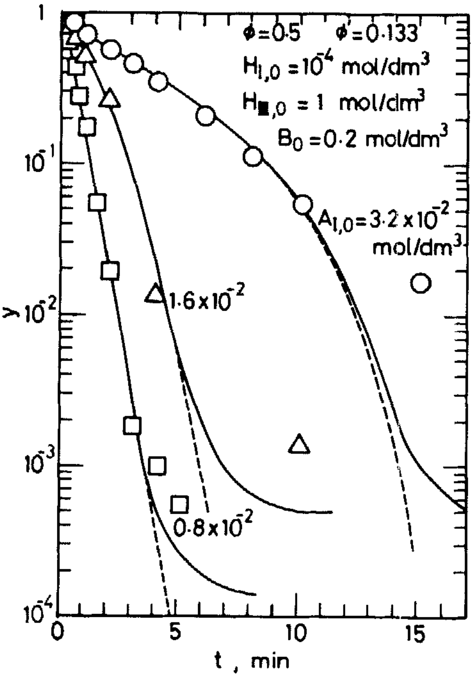

FIG. 6. Effect of the initial concentration of copper in the external phase on y vs time relation.

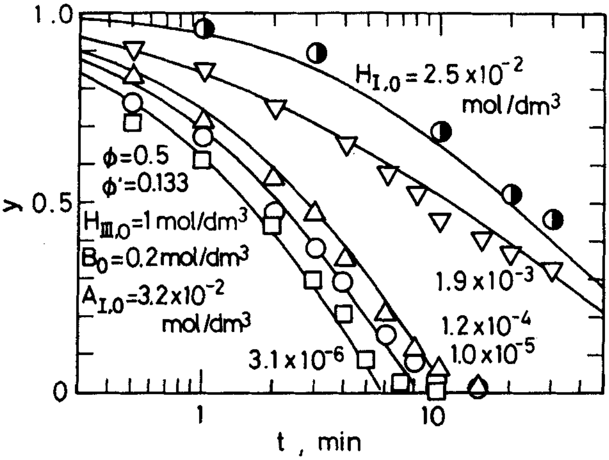

FIG. 7. Effect of the initial hydrogen ion concentration in the external phase on the extraction rate.

the initial concentration of copper, the lower the degree of removal, indicating that the process is nonlinear with respect to the copper concentration. This may be explained as follows. When $A_{I,0}$ is higher, the internal droplets in the peripheral region of the drop are more rapidly saturated with copper, and the complex must diffuse through Phase II to the more inner region of the drop to release copper in Phase III, suggesting that the internal mass transfer resistance is important. On the other hand, when $A_{I,0}$ is low, the external mass transfer is rate controlling, and $-dy/dt$ is much higher than when $A_{I,0}$ is high.

Effect of Hydrogen Ion Concentration in the Feed Solution

The pH of the external phase is closely connected with the forward reaction rate and the distribution ratio of copper. In the extraction of copper from leach liquors, the pH of the feed solutions is below 3. In this study, however, pH was varied in the range from 1.6 to 5.5 to investigate the effect of the reaction rate on the extraction rate and how the rate-determining step changes with pH. The effect of the initial hydrogen ion concentration is shown in Fig. 7. As anticipated from Eq. (3), the higher $H_{I,0}$, the lower the extraction rate. Under the condition of high $H_{I,0}$, the rate of complex formation at the interface of the drop is slow, and this step is rate determining. On the other hand, when $H_{I,0}$ is low, the reaction rate is fast,

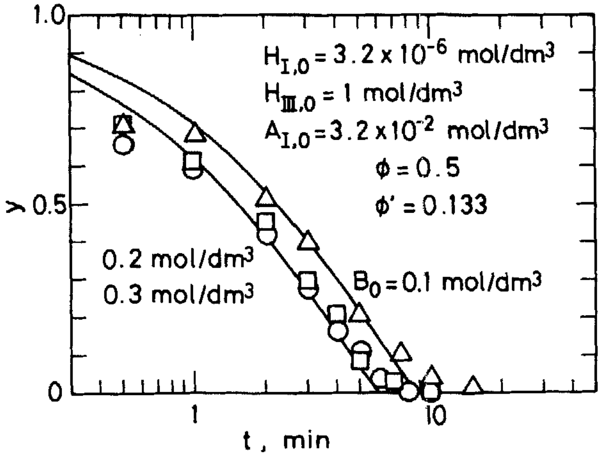

FIG. 8. Effect of the carrier concentration on the extraction rate.

and $H_{I,0}$ has little influence on the rate. The difference in the rate observed at high pH is mainly due to the difference in drop size. In this range of pH, diffusion through the peripheral oil layer and the internal diffusion limit the extraction rate.

Effect of Carrier Concentration

Figure 8 shows the effect of the carrier concentration B_0. The rate when B_0 is 0.2 *M* is slightly higher than that when B_0 is 0.1 *M*. However, a further increase in B_0 does not result in an increase in the rate. This is because the viscosity of the membrane phase increases with increasing B_0. The viscosities are 3.0, 3.4, and 4.2 cP when B_0's are 0.1, 0.2, and 0.3 mol/dm^3, respectively. The increase in viscosity makes the drop diameter large, the diffusivity of the complex low, and the internal resistance more important.

Effect of Hydrochloric Acid Concentration in the Internal Aqueous Phase

Figure 9 shows how the extraction rate varies with the concentration of hydrochloric acid in the internal phase. The rate increases with increasing $H_{III,0}$ because the capacity of the internal phase as a sink for copper

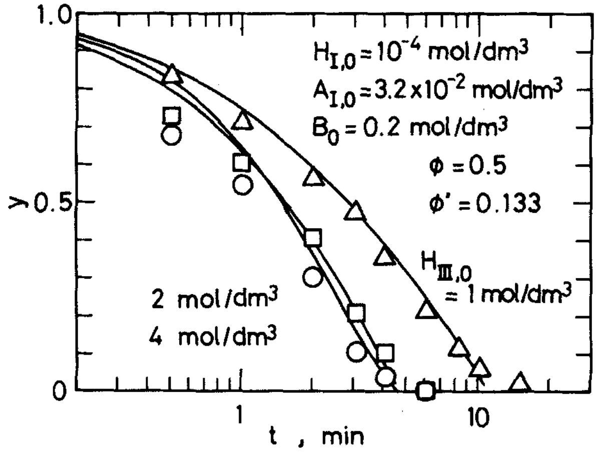

FIG. 9. Effect of the initial concentration of hydrochloric acid in the internal phase on the extraction rate.

increases. However, the degree of the increase becomes small when $H_{III,0}$ is higher than 2 mol/dm^3. This is because the emulsion becomes very viscous, resulting in a large dispersed emulsion drop when $H_{III,0}$ is as high as 4 mol/dm^3.

Effect of Volume Fraction of the Internal Aqueous Phase

Figure 10 shows the effect of ϕ, the volume fraction of the internal aqueous phase on the Sauter mean diameter of the W/O emulsion drop. With increasing ϕ, the viscosity of the emulsion phase and also the drop diameter increase. As shown in Fig. 11, the increase in the drop diameter lowers the extraction rate in spite of the increase in the capacity for trapping copper with increasing ϕ.

Effect of Stirring Speed

The effect of stirring speed on the drop diameter is shown in Fig. 12. The diameter is proportional to $n^{-1.2}$ in accordance with the previous work (*30*). Thus, as shown in Fig. 13, the extraction rate increases with increasing stirring speed.

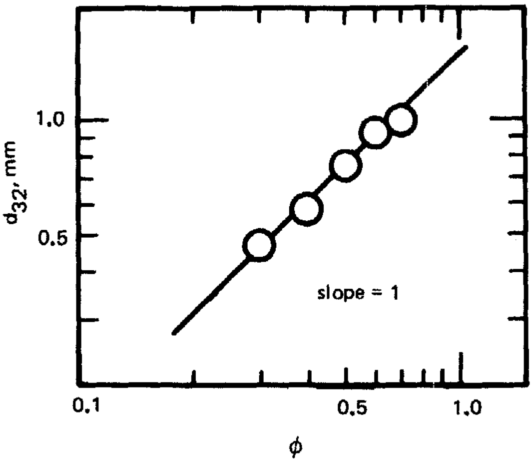

FIG. 10. Effect of the volume fraction ϕ on the Sauter mean diameter of W/O emulsion drop.

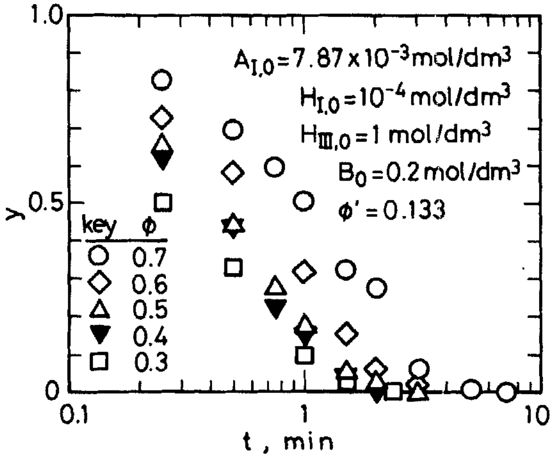

FIG. 11. Effect of the volume fraction ϕ on the extraction rate.

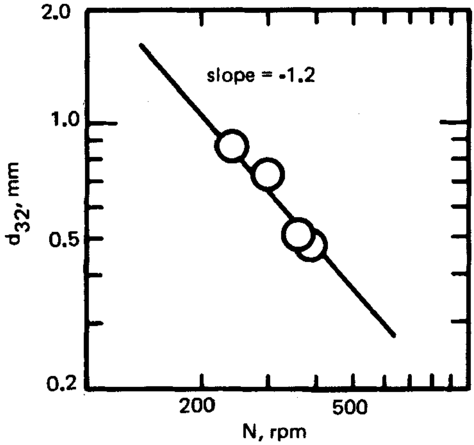

FIG. 12. Effect of stirring speed on the Sauter mean diameter of W/O emulsion drop.

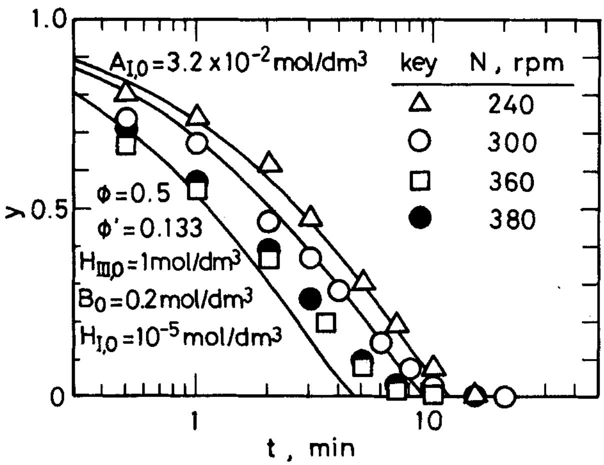

FIG. 13. Effect of stirring speed on the extraction rate.

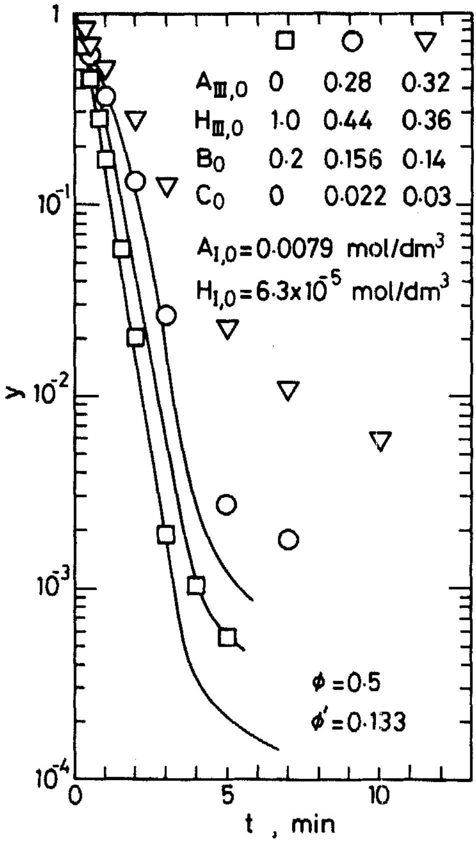

FIG. 14. Effect of the preloading on the extraction rate.

Effect of Preloading of Copper in the Internal Aqueous Phase

In liquid surfactant membrane processes, most of the emulsion leaving the settler which separates the emulsion phase from the external phase is recycled to the extraction vessel without demulsifying it, and only a small portion of the emulsion is demulsified. Therefore, the drop, already containing a considerable amount of copper both in the membrane and the internal phase, is brought into contact with the feed solution. A series of experiments was conducted using the "preloaded emulsion" to examine the effect of the copper concentration in the internal phase. To prepare the emulsion phase, a mixed solution of $CuCl_2$ and HCl was emulsified with the total concentration of Cl^- kept constant at 1 mol/dm^3. As seen in Fig. 14, the

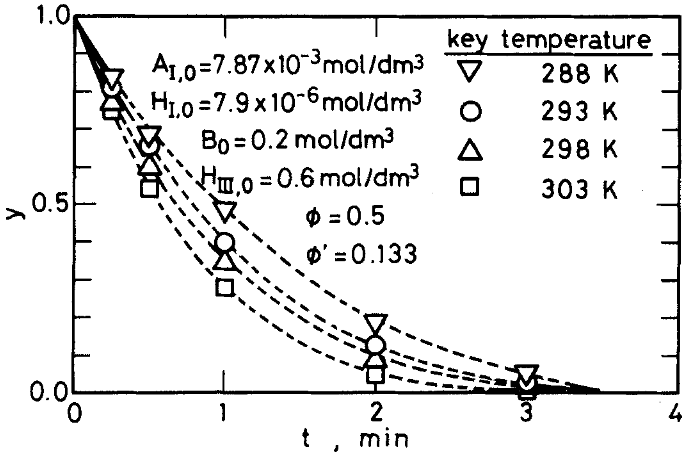

FIG. 15. Effect of temperature on the extraction rate.

extraction rate decreased with an increase in $A_{III,0}$. However, about 99.5% of the copper was rapidly removed even when $A_{III,0}$ was 0.32 mol/dm^3, and the concentration ratio A_{III}/A_I was as high as 25,000.

Effect of Temperature

As shown in Fig. 15, the rate increased with increasing temperature. The apparent activation energy was calculated as 6.5 kcal/mol from the rates at 50% extraction. This value suggests that the diffusion rate rather than the reaction rate is rate determining.

Effect of Internal Drop Diameter

The effect of R_μ, the Sauter mean diameter of the internal droplets, is shown in Fig. 16. As described in a previous paper (*13*), R_μ was controlled by adjusting the intensity of the sonication. R_μ is related to the interfacial area between Phase II and Phase III where the stripping reaction (4) occurs. As shown in Fig. 16, the rate was not influenced by R_μ, indicating that the stripping reaction was sufficiently fast. This means that as long as the emulsion is stable, large internal droplets are favorable in view of process economics because demulsification is extremely difficult when R_μ is small.

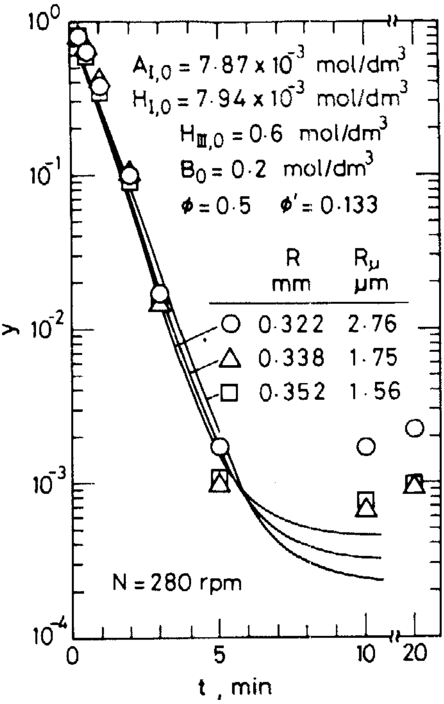

FIG. 16. Effect of the droplet diameter of the internal phase on the extraction rate.

DISCUSSION

Comparison of the Experimental Results with the Computed Results

The computed time courses of extraction were obtained on the basis of the present permeation model, and are shown by the solid lines in the above figures. The effective diffusivity $D_{e,B}$ was determined so that the best agreement between the experimental and the calculated results might be obtained. The effect of viscosity on $D_{e,B}$ was also considered by assuming that D_e is inversely proportional to the membrane viscosity as shown in Table 1. When $H_{I,0}$ was considerably high and the buffer solution was not used, H_I increased considerably during the experiment. For example, H_I increased from an initial value of 0.0019 to 0.035 in 20 min. In this case the change in H_I monitored by a pH meter was taken into account in the calculation. It can be seen in these figures that agreement between the experimental and the computed results is fairly good if we consider that most of the parameters were determined by independent experiments. However, the data obtained under the condition that the concentration of the complex in the membrane was high, i.e., when $A_{\mathrm{I},0}$ or $A_{\mathrm{III},0}$ was high, could not be satisfactorily simulated by the present model. For example, the model gave a considerably higher rate than the observed result in the later stage of the extraction when $A_{\mathrm{I},0}$ was 0.032 mol/dm^3 as shown in Fig. 6. This tendency is also seen in Fig. 14. This point needs to be examined further.

The bulk diffusivity of B, D_B, was estimated as $8.48 \times 10^{-6}/\mu$ cm^2/s by the Wilke-Chang equation. Here μ is the viscosity of the membrane phase expressed in cP. It was confirmed that μ did not change appreciably by the formation of the complex in the organic phase if the total concentration of the carrier was kept constant. The ratio $D_{e,B}/D_B$ is about 0.24. This value is considerably smaller than 0.44, the lowest value predicted by the Russel equation (*13, 15, 31*) on the assumption that there is no diffusion contribution in the internal aqueous phase to transport in the emulsion drop. Although the reason of this discrepancy is not clear, it may be due to the errors in estimating D_B in the solution of high concentration and $D_{e,B}$.

Effect of the Membrane Breakup on the Degree of Extraction

The leakage of the internal phase containing a high concentration of copper to the external phase lowers the degree of the removal of copper. As shown in Fig. 6, y becomes much lower as the initial copper concentration decreases. The equilibrium concentration of copper, which is the lowest concentration attained when the extraction proceeds ideally without breakup and the swelling of the drop caused by water permeation due to osmotic pressure, can be calculated from the material balance and the equilibrium equations:

$$A_{\mathrm{I},0}V_{\mathrm{I}} + C_0 V_{\mathrm{II}} + A_{\mathrm{III},0}V_{\mathrm{III}} = A_{\mathrm{I},e}V_{\mathrm{I}} + C_e V_{\mathrm{II}} + A_{\mathrm{III},e}V_{\mathrm{III}} \tag{20}$$

$$B_0 + 2C_0 = B_e + 2C_e \tag{21}$$

$$2A_{\mathrm{III},0} + H_{\mathrm{III},0} = 2A_{\mathrm{III},e} + H_{\mathrm{III},e} \tag{22}$$

$$K_{ex} = C_e H_{\mathrm{I},e}^2 / A_{\mathrm{I},e} B_e^2 = C_e H_{\mathrm{III},e}^2 / A_{\mathrm{III},e} B_e^2 \tag{23}$$

The values of y_e $(= A_{\mathrm{I},e}/A_{\mathrm{I},0})$ calculated by Eqs. (20)–(23) were as low as 4.9×10^{-10}, 8.5×10^{-10}, and 1.2×10^{-9} when $A_{\mathrm{I},0}$ were 0.008, 0.016, and 0.032 mol/dm^3, respectively. Here, H_{I} at $t = 10$ min was used as $H_{\mathrm{I},e}$. These

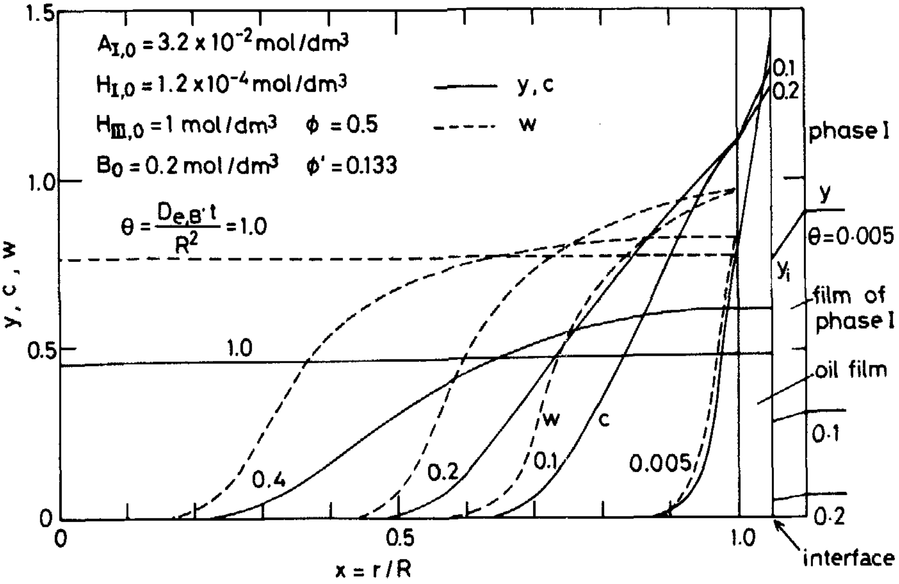

FIG. 17. Computed concentration profiles in W/O/W multiphase system.

values of y_e are much smaller than the experimentally observed lowest values. This is partly due to leakage of the internal phase. The dotted lines in Fig. 14 represent the computed results when leakage is not considered. On the other hand, the solid lines are the results when leakage is taken into account. It was also found that if $A_{\mathrm{III},av}$, the average concentration of copper in the internal aqueous phase, is used instead of $(A_{\mathrm{III}})_{r=R'}$ in Eq. (5), the effect of the leakage predicted by the present model is much smaller because $A_{\mathrm{III},av}$ is also much smaller than $(A_{\mathrm{III}})_{r=R'}$ as can be seen from Fig. 17 which shows the computed concentration profiles in the drop. It is also noted that the value of $(A_{\mathrm{III}})_{r=R'}$ is always kept large during extraction. Thus it may be deduced that the internal phase in the peripheral region of the W/O emulsion drop leaks.

It can be seen in Fig. 16 that the lowest value of y for $R_\mu = 2.76$ μm is higher than that of $R_\mu = 1.75$ or 1.56 μm. This is because the W/O emulsion drop is more stable when R_μ is smaller. The values of v_b were 4.9×10^{-4}, 3.3×10^{-4}, and 2.5×10^{-4} cm^3/s when the R_μ's were 2.76, 1.75, and 1.56 μm, respectively.

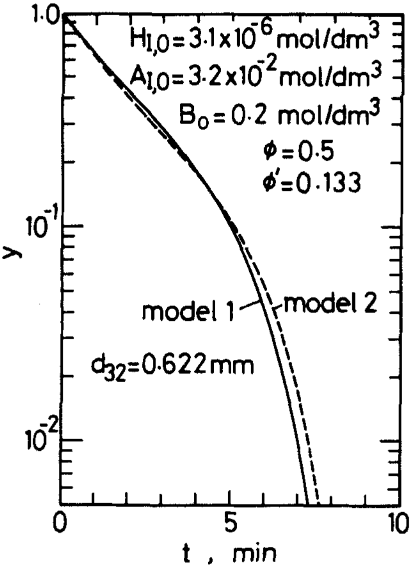

FIG. 18. Comparison of the uniform drop size distribution model with the model in which the drop size distribution is considered.

Effect of the Drop Size Distribution on the Extraction Rate

The present model was extended to the case where the drop size distribution of the emulsion phase exists by a method similar to that described in a previous paper (*13*). Comparison of the results computed by the present model (Model 1) with those by the model where the drop size distribution is considered (Model 2) is shown in Fig. 18. Here, the experimentally measured drop size distribution was used in the calculation. The solid line represents the result by Model 1 where the Sauter mean diameter was used as the average diameter. It is seen that the results from these models roughly agree with each other, indicating that the present model can be used to predict the extraction rate if d_{32} is used as a characteristic drop diameter.

Simulation of the Experimental Data by a Complete Mixing Model

One of the characteristics of the present model is that the degree of convection in the W/O emulsion drop can be varied by assigning the

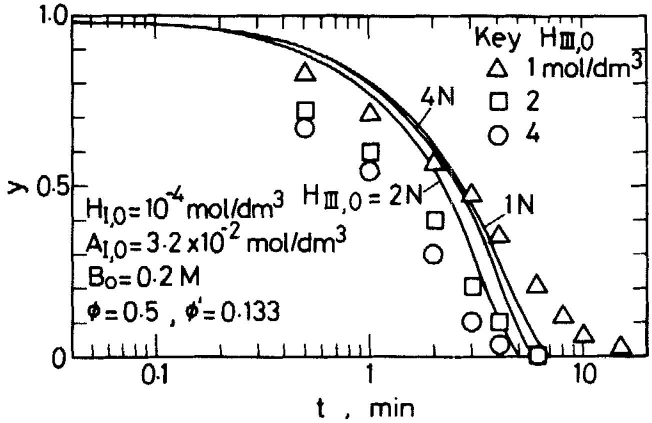

FIG. 19. Simulation of the experimental data by the complete mixing model.

appropriate value to D_e. If considerable convection exists in the drop, the mass transfer resistance can be ignored. This situation corresponds to a very large value of D_e and, in turn, a very small value of Bi. Then, the basic equations for the complete mixing model (Model 3) are represented as follows:

$$-V_I dA_I/dt = k_A S(A_I - A_{I,i}) \tag{24}$$

$$V_{II} dB/dt = k_B S(B_i - B) + 2k_r S_\mu(CH_{III} - K_{ex}A_{III}B^2/H_{III}) \tag{25}$$

$$V_{II} dC/dt = k_C S(C_i - C) - k_r S_\mu(CH_{III} - K_{ex}A_{III}B^2/H_{III}) \tag{26}$$

$$V_{III} dA_{III}/dt = k_r S_\mu(CH_{III} - K_{ex}A_{III}B^2/H_{III}) \tag{27}$$

$$\text{I.C.;} \quad A_I = A_{I,0},\ A_{III} = A_{III,0},\ B = B_0,\ C = C_0,\ (H_{III} = H_{III,0}) \tag{28}$$

Additional conditions are as follows:

$$\begin{aligned} k_A(A_I - A_{I,i}) &= k_f(A_{I,i}B_i/H_{I,i} - C_iH_{I,i}/K_{ex}B_i) \\ &= k_B(B - B_i)/2 \\ &= k_C(C_i - C) \end{aligned} \tag{29}$$

$$2A_{III,0} + H_{III,0} = 2A_{III} + H_{III} \tag{30}$$

The dimensionless parameters to be specified are

$$m_{A,\mathrm{I}} = A_{\mathrm{I},0}/B_0,\ m_{A,\mathrm{III}} = 2A_{\mathrm{III},0}/B_0,\ m_{H,\mathrm{I}} = H_{\mathrm{I},0}/B_0,\ m_{H,\mathrm{III}} = H_{\mathrm{III},0}/B_0,$$
$$n_B = k_B/k_A,\ n_C = k_C/k_A,\ n_f = k_f/k_A,\ \gamma = k_r H_{\mathrm{III},0} R/(3k_A R_\mu),\ K_{ex},$$
$$\tau = k_A(S/V_T)t = 3k_A\phi' t/R,\ \phi,\ \phi' \tag{31}$$

Figure 19 shows the comparison between the experimental results and the computed results by the complete mixing model. The data are the same as those shown in Fig. 9. It is seen that the effect of $H_{\mathrm{III},0}$ cannot be explained by Model 3, suggesting that the internal diffusion must be considered in analyzing the permeation rate.

Permeation Model When Phase II Is in Chemical Equilibrium with Phase III ($q = \infty$)

When the parameter q is sufficiently large, the internal aqueous phase is considered to be in chemical equilibrium with the oil membrane phase. In this case the diffusion equations in the W/O emulsion drop are represented as follows:

$$(1-\phi)\frac{\partial C}{\partial t} + \phi\frac{\partial A_{\mathrm{III}}}{\partial t} = D_{e,C}\left(\frac{\partial^2 C}{\partial r^2} + \frac{2}{r}\frac{\partial C}{\partial r}\right) \tag{32}$$

$$(1-\phi)\frac{\partial B}{\partial t} + 2(1-\phi)\frac{\partial C}{\partial t} = D_{e,B}\left(\frac{\partial^2 B}{\partial r^2} + \frac{2}{r}\frac{\partial B}{\partial r}\right) + 2D_{e,C}\left(\frac{\partial^2 C}{\partial r^2} + \frac{2}{r}\frac{\partial C}{\partial r}\right) \tag{33}$$

$$K_{ex} = \frac{CH_{\mathrm{III}}^2}{A_{\mathrm{III}}B^2} = \frac{C(2A_{\mathrm{III},0} + H_{\mathrm{III},0} - 2A_{\mathrm{III}})^2}{A_{\mathrm{III}}B^2} \tag{34}$$

The numerical solutions of Eqs. (5) and (32)–(34) under the conditions of Eqs. (9)–(13) were obtained and compared with those for the finite values of q. It was found that under the experimental condition indicated in Fig. 16, the solutions for q greater than 0.5 agree with those for $q = \infty$. However, if q is smaller than 0.01, the stripping step becomes rate determining.

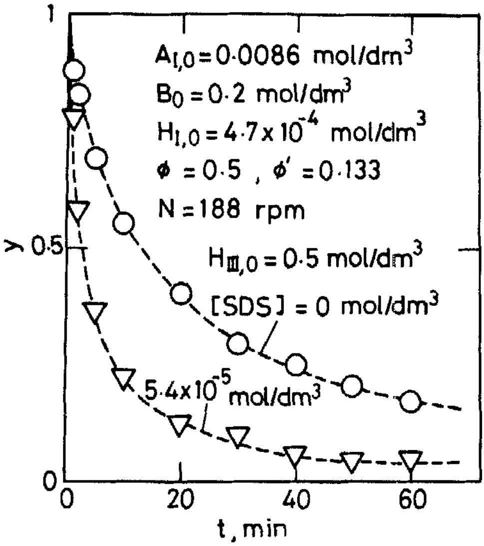

FIG. 20. Effect of addition of anionic surfactant on the extraction rate.

Effect of Addition of Anionic Surfactant to the External Phase

As described above, it was deduced that the reaction at the interface between the external aqueous phase and the W/O emulsion drops are rate determining when $H_{I,0}$ is considerably high. Therefore, under this condition the rate of the extraction may be increased by increasing the rate of the interfacial reaction. It was anticipated that an anionic surfactant added to the external aqueous phase is adsorbed at the aqueous–organic interface, and the interface has a negative charge. Then the interface attracts cupric ions by the electric force, resulting in a much higher copper concentration at the interface than in the bulk liquid. Hydrogen ion may also be concentrated at the interface. However, the divalent cupric ion is more concentrated at the interface than the univalent hydrogen ion. Thus, the concentration ratio $[Cu^{2+}]/[H^+]$ at the interface is higher than in the bulk liquid. Because the interfacial reaction is proportional to $[Cu^{2+}]/[H^+]$ as indicated by Eq. (3), the extraction rate increases by adding anionic surfactants to the feed solution. As shown in Fig. 20, the rate was remarkably enhanced by the addition of a very small amount of sodium dodecyl sulfate.

CONCLUSION

Comprehensive experimental data on the batch extraction of copper by liquid surfactant membranes using a chelating agent, SME529, as a carrier were analyzed on the basis of a general permeation model in which the diffusion in the W/O emulsion drop, the external mass transfer around the drop, the rates of the formation, as well as the decomposition of the complex at the aqueous-organic interface and the leakage of the internal phase to the external phase due to the membrane breakup were taken into account. It was found that the effects of various experimental conditions such as concentrations of copper and hydrogen ion in the internal and the external phases, the carrier concentration, the drop diameter, and the temperature on the extraction rate could be simulated by the present model. It was also found from a comparison of the present model and the complete mixing model that the mass transfer resistance in the W/O emulsion drop must be taken into account to explain the behavior of the permeation quantitatively. The present model may be easily extended to cases where different types of carriers and interfacial reactions are involved.

SYMBOLS

A	concentration of copper (mol/dm^3 or mol/cm^3)
a_0	specific interfacial area between external aqueous phase and W/O emulsion drops (cm^{-1})
B	concentration of chelating agent (mol/dm^3 or mol/cm^3)
b	B/B_0
Bi	Biot number ($= k_A R/D_{e,B}$)
C	concentration of complex (mol/cm^3 or mol/cm^3)
c	$2C/B_0$
D	molecular diffusivity (cm^2/s)
D_e	effective diffusivity in W/O emulsion drop (cm^2/s)
d_{32}	Sauter mean diameter of W/O emulsion drop (cm)
f	fraction of volume of internal aqueous phase which leaks to external aqueous phase due to membrane breakup
H	concentration of hydrogen ion (mol/dm^3)
K_A	overall mass transfer coefficient defined by Eq. (16) (cm/s)
K_{ex}	extraction constant
k_A, k_H	mass transfer coefficients of Cu^{2+} and H$^+$ through external aqueous stagnant film, respectively (cm/s)

k_B, k_C	mass transfer coefficients of carrier and complex through the oil layer around W/O emulsion drop, respectively (cm/s)
k_f, k_r	forward and reverse reaction rate constants, respectively (cm/s), ($\mathrm{cm}^4/\mathrm{mol}\cdot\mathrm{s}$)
m	initial concentration ratio defined by Eq. (14) or Eq. (31)
N	stirring speed (rpm)
n_J	k_J/k_A ($J = B$, C, and f)
q	$Rk_rH_{\mathrm{III},0}/R_\mu k_A$
R	radius of W/O emulsion drop (cm)
R'	$R - \delta$ (cm)
R_μ	radius of internal droplet (cm)
r	radial distance (cm)
r_{CB}	$D_{e,C}/D_{e,B}$ or D_C/D_B
r_f, r_r	rates of extraction and stripping, respectively, ($\mathrm{mol}/\mathrm{cm}^2\cdot\mathrm{s}$)
S	total interfacial area between external aqueous phase and W/O emulsion drops (cm^2)
S_μ	total interfacial area between organic membrane phase and internal aqueous droplet (cm^2)
t	time (s)
V	volume (cm^3 or dm^3)
v_b	volumetric rate of leakage of internal phase to external phase due to membrane breakup (cm^3/s)
w	$2A_{\mathrm{III}}/H_{\mathrm{III},0}$
x	r/R
y	$A_{\mathrm{I}}/A_{\mathrm{I},0}$

Subscripts

0	initial value
A	copper
B	chelating agent
C	complex
H	hydrogen ion
i	interface between external aqueous phase and W/O emulsion drop
I	Phase I (external aqueous phase)
II	Phase II (organic membrane phase)
III	Phase III (internal aqueous phase)
e	value at equilibrium
T	total value

Greeks

α	$Rv_b/k_A V_T$
γ	$k_r H_{\mathrm{III},0} R/(3k_A R_\mu)$
δ	thickness of oil layer around W/O emulsion drop (cm)
μ	viscosity of Phase II, (cP)
τ	$k_A(S/V_T)t$
ϕ	volume fraction of Phase III in W/O emulsion drop ($= V_{\mathrm{III}}/(V_{\mathrm{II}} + V_{\mathrm{III}})$)
ϕ'	volume fraction of W/O emulsion in W/O/W multiphase emulsion ($=(V_{\mathrm{II}} + V_{\mathrm{III}})/V_{\mathrm{T}}$)
θ	$D_{e,B}t/R$

Acknowledgments

This work was supported by a Grant-in-Aid for Special Research Project on Environmental Science from the Ministry of Education, Culture and Science, Japan, in 1982 (No. 57030054). We thank the Shell Chemical Co., Ltd., for offering SME529 and Dispersol.

REFERENCES

1. N. N. Li, U.S. Patent 3,410,794 (1968).

2. N. N. Li, *AIChE J.*, *17*, 459 (1971).

3. N. N. Li, *Ind. Eng. Chem., Process. Des. Dev.*, *10*, 215 (1971).

4. N. D. Shah and T. C. Owens, *Ind. Eng. Chem., Prod. Res. Dev.*, *11*, 58 (1972).

5. R. P. Cahn and N. N. Li, *J. Membrane Sci.*, *1*, 129 (1976).

6. G. Casamatta, C. Chavarie, and H. Angelino, *AIChE J.*, *24*, 945 (1978).

7. P. Alessi, I. Kikic, and M. Orlandini-Visalberghi, *Chem. Eng. J.*, *19*, 221 (1980).

8. W. Halwachs, E. Flaschel, and K. Schügerl, *J. Membrane Sci.*, *6*, 33 (1980).

9. V. J. Kremesec, Jr., and J. C. Slattery, *AIChE J.*, *28*, 492 (1982).

10. N. N. Li and A. L. Shrier, *Recent Developments in Separation Science*, Vol. 1, CRC Press, Boca Raton, Florida, 1972, p. 163.

11. R. P. Cahn and N. N. Li, *Sep. Sci.*, *9*, 505 (1974).

12. W. S. Ho., T. A. Hatton, E. N. Lightfoot, and N. N. Li, *AIChE J.*, *28*, 662 (1982).

13. M. Teramoto, H. Takihana, M. Shibutani, T. Yuasa, and N. Hara, *Sep. Sci. Technol.*, *18*, 397 (1983).

14. T. Kitagawa, Y. Nishikawa, J. W. Frankenfeld, and N. N. Li, *Environ. Sci. Technol.*, *11*, 602 (1977).

15. M. Teramoto, H. Takihana, M. Shibutani, T. Yuasa, Y. Miyake, and H. Teranishi, *J. Chem. Eng. Jpn.*, *14*, 122 (1981).

16. E. L. Cussler, D. F. Evans, and M. A. Matesich, *Science*, *172*, 377 (1971).

17. A. M. Hochhauser and E. L. Cussler, *AIChE Symp. Ser., 71*, 136 (1975).
18. E. S. Matulevicius and N. N. Li, *Sep. Purif. Methods, 4*, 73 (1975).
19. T. P. Martin and G. A. Davies, *Hydrometallurgy, 2*, 315 (1976/1977).
20. J. W. Frankenfeld and N. N. Li, *Recent Developments in Separation Science*, Vol. 3, CRC Press, Boca Raton, Florida, 1977.
21. K.-H. Lee and E. L. Cussler, *AIChE J.*, 24, 860 (1978).
22. W. Völkel, W. Halwachs, and K. Schügerl, *J. Membrane Sci.*, 6, 19 (1980).
23. J. Strzelbicki and W. Charewicz, *Hydrometallurgy, 5*, 243 (1980).
24. J. W. Frankenfeld, R. P. Cahn, and N. N. Li, *Sep. Sci. Technol., 16*, 385 (1981).
25. R. Marr and A. Kopp, *Chem. Ing. Tech., 52*, 399 (1980).
26. Y. Miyake, Y. Takenoshita, and M. Teramoto, *J. Chem. Eng. Jpn., 16*, 203 (1983).
27. Y. Miyake, A. Mitsumoto, and M. Teramoto, Unpublished Work.
28. P. H. Calderbank and M. B. Moo-Young, *Chem. Eng. Sci., 16*, 39 (1961).
29. C. R. Wilke and P. Chang, *AIChE J., 1*, 264 (1955).
30. T. Vermeulen, G. M. Williams, and G. E. Langlios, *Chem. Eng. Prog., 51*, 85-F (1955).
31. H. W. Russel, *J. Am. Ceram. Soc., 18*, 1 (1954).

Received by editor February 14, 1983